CVI
Journals.ASM.org

Antigen Targeting to Major Histocompatibility Complex Class II with Streptococcal Mitogenic Exotoxin Z-2 M1, a Superantigen-Based Vaccine Carrier

Fiona J. Radcliff,[a] Jacelyn M. S. Loh,[a] Birgit Ha,[a]* Diana Schuhbauer,[a,b]* James McCluskey,[b] and John D. Fraser[a]

School of Medical Sciences and Maurice Wilkins Centre for Molecular Biodiscovery, University of Auckland, Auckland, New Zealand,[a] and Department of Microbiology & Immunology, The University of Melbourne, Melbourne, Australia[b]

Streptococcal mitogenic exotoxin Z-2 (SMEZ-2) is a streptococcal superantigen that primarily stimulates human T cells bearing Vβ8 and mouse T cells bearing Vβ11. Mutagenesis of T cell receptor (TCR)-binding residues (W75L, K182Q, D42C) produced a mutant called M1 that was $>10^5$-fold less active toward human peripheral blood lymphocytes and splenocytes from transgenic mice that express human CD4 and either human HLA-DR3-DQ2 or HLA-DR4-DQ8. Similarly, cytokine production in response to M1 in lymphocyte culture was rendered undetectable, and no change in the frequency of Vβ11-bearing T cells in mice receiving M1 was observed. M1 toxoid was tested as a potential vaccine conjugate. Vaccination with 1 to 10 μg M1 conjugated to ovalbumin (M1-ovalbumin) resulted in more rapid and quantitatively higher levels of anti-ovalbumin IgG, with endpoint titers being 1,000- to 10,000-fold greater than those in animals immunized with unconjugated ovalbumin. Substantially higher levels of anti-ovalbumin IgG were observed in mice transgenic for human major histocompatibility complex (MHC) class II. Substitution of M1 with an MHC class II binding mutant (DM) eliminated enhanced immunity, suggesting that M1 enhanced the delivery of antigen via MHC class II-positive antigen-presenting cells that predominate within lymphoid tissue. Immunization of animals with a conjugate consisting of M1 and ovalbumin peptide from positions 323 to 339 generated levels of anti-peptide IgG 100-fold higher than those in animals immunized with peptide alone. Coupling of a TCR-defective superantigen toxoid presents a new strategy for conjugate vaccines with the additional benefit of targeted delivery to MHC class II-bearing cells.

Superantigens from *Streptococcus pyogenes* are a structurally conserved family of proteins (16) with the common ability to cross-link major histocompatibility complex (MHC) class II outside the peptide binding domain and the T cell receptor (TCR), causing massive T cell proliferation and systemic cytokine-mediated shock (11, 25). Superantigens are highly mitogenic to T cells from many species, but sensitivity and toxicity are typically reduced by several orders of magnitude in mice compared to humans (33). To better mimic the extreme sensitivity of human to superantigens, mice transgenic for human HLA genes that recapitulate many of the symptoms of superantigen-mediated human toxinosis have been used (10, 35, 39, 46).

Bacterial superantigens have evolved over time to become exquisitely specific for components of the human immune system, raising the possibility that with appropriate modification they could be used as the basis for immune-targeting therapeutics in the same way that tetanus toxoid and other toxoids have been used with great success in conjugate vaccines (1, 15). The specificity of superantigens for MHC class II is of particular interest, as MHC class II is a molecule expressed on professional antigen-presenting cells such as dendritic cells (DCs), B cells, and macrophages. MHC class II is central to the initiation of antigen-specific immune responses by $CD4^+$ T helper cells and the subsequent development of humoral and cellular immunity. Immature antigen-presenting cells, particularly dendritic cells, continually cycle MHC class II between the cell membrane and endosomes, where antigen sampling determines whether the endosome contents go on to late endosomes/multivesicular bodies or lysosomes or are recycled (43). Targeting antigens directly to the MHC class II pathway enables delivery of material directly into the antigen-processing pathway of antigen-presenting cells. This approach has been tested using antibody (Ab) specific for MHC class II (6) or with Troybodies, recombinant MHC class II antibodies which have been modified to incorporate MHC class II-restricted T cell epitopes (29).

To establish whether a TCR-defective superantigen toxoid might enhance immunogenicity of coupled antigens by MHC class II targeting, we modified the most potent superantigen from *S. pyogenes*, streptococcal mitogenic exotoxin Z-2 (SMEZ-2) (33), to produce a mutant (M1). The M1 protein targets all subsets of dendritic cells in the mouse and is highly effective at eliciting an enhanced cellular response to coupled antigen both *in vitro* and *in vivo* when administered in conjunction with the adjuvant α-galactosylceramide (13). We have thoroughly characterized the M1 protein to confirm that it is defective in TCR binding and devoid of *in vitro* and *in vivo* superantigen activity. *In vivo* studies designed to further assess the safety and utility of M1 *in vivo* demonstrated that conjugating antigen to M1 stimulated significantly enhanced antibody responses in both wild-type and sensitive humanized transgenic mice expressing human HLA-DR3-DQ2 or HLA-DR4-DQ8.

Received 3 September 2011 **Returned for modification** 22 October 2011
Accepted 23 January 2012
Published ahead of print 1 February 2012
Address correspondence to John D. Fraser, jd.fraser@auckland.ac.nz.
* Present address: B. Ha, Plant & Food Research Mt. Albert, Auckland, New Zealand; D. Schuhbauer, Hoffmann-La Roche Ltd., Basel, Switzerland.

doi:10.1128/CVI.05446-11

TABLE 1 Sets of mismatched primers used to create the M1, M2, and DM mutants of SMEZ-2

Mutation	Primer sequence
W75L[a,b]	5′-CCATTTGATTTGAACTATTTATC-3′
	5′-GATAAATAGTTCAAATCAAATGG-3′
K182Q[a,b]	5′-GATATAGAGATCAAGAAAGTATC-3′
	5′-GATACTTTCTTGATCTCTATATC-3′
D42C1[a,b,c]	5′-GATGTTAGATGTGCTAGAGATTTC-3′
	5′-CTCTAGCACATCTAACATCAAGTTTC-3′
Y18A[b,c]	5′-CGATTGTAGCTGAATATTCAGATATAG-3′
	5′-GAATATTCAGCTACAATCGTACTATAG-3′
H202A.D204A[c]	5′-GGGGCTTTAGCTATAGAAATTGACTCC-3′
	5′-AGCTAAAGCCCCAATTTTATCTATATTG-3′

[a] SMEZ-2 M1 mutant was created by mutating 3 TCR-binding residues (W57L, K182Q, D42C). This mutant bound to MHC class II but not the TCR.
[b] SMEZ-2 M2 mutant was created by mutating 4 TCR-binding residues (Y18A, W75L, K182Q, D42C). This mutant bound to MHC class II but not the TCR.
[c] SMEZ-2 DM mutant was created by mutating two TCR-binding residues (Y18A, D42C) and two MHC class II-binding residues (H202A, D204A). This mutant no longer bound to MHC class II or the TCR.

MATERIALS AND METHODS

Superantigens. Cloning and sequencing of the *smez-2* gene encoding SMEZ-2 from *S. pyogenes* strain 2035 have been described elsewhere (33). Mutations in the TCR or MHC class II binding sites were introduced by site-directed mutagenesis using pGEX utility primers (5′-TCAGAGGTT TTCACCGTC-3′ and 5′-ACCATCCTCCAAAATCGG-3′) and sets of mismatched overlapping primers in a two-step overlap PCR (17) (Table 1). Overlap PCR products were cloned into the pGEX-3C expression vector using the restriction enzyme sites included in the pGEX utility primers. Genes were sequenced and expressed in *Escherichia coli* DH5α cells as glutathione *S*-transferase fusion proteins. Cultures were grown at 28°C in Terrific broth and induced for 3 to 4 h after adding 0.1 mM isopropyl-β-D-thiogalactopyranoside (IPTG). Two-step purification involved affinity chromatography using glutathione agarose, cleavage with 3C protease, and finally, cation-exchange chromatography using carboxymethyl Sepharose (Amersham Pharmacia, United Kingdom) as described previously (33).

Site-specific mutagenesis of amino acid residues critical to TCR binding in SMEZ-2 were inferred by structural analogy to similar positions in the structure of staphylococcal enterotoxin C3 (SEC3) cocrystallized with TCR (26). A combination of two amino acid mutants (W75L, K182Q) showed greater than 5 orders of magnitude less potency than the parent molecule in human T cell stimulation assays. These were combined with a third mutation that replaced position D42 with a cysteine. This residue was chosen because it is highly solvent exposed and central to the TCR binding site, making it ideal for direct coupling of peptides and proteins well away from the MHC class II binding site located on the opposite face of the SMEZ-2 molecule (Fig. 1).

Expression and purification of Vβ8.1/Vα1.2 TCR and HLA-DR1. The *Drosophila melanogaster* S2 cell line was transfected with calcium phosphate/DNA crystals using 10 μg pRmHa-3 Vβ8 and pRmHa-3 Vα1.2 DNA each (5) and 1 μg of pBS-hsPuro DNA (from Klaus Karjaleinen, Basel Institute for Immunology, Basel, Switzerland). Resistant cells were selected with 100 μg/ml puromycin (Sigma-Aldrich, Sydney, Australia). Expression of the soluble, native Vβ8 TCR was confirmed by intracellular fluorescence-activated cell sorter (FACS) analysis and by enzyme-linked immunosorbent assay (ELISA). After induction of expression with 1 mM copper sulfate, S2 cell supernatants were concentrated with 40% (vol/vol) saturated $(NH_4)_2SO_4$. After dialysis into phosphate-buffered saline (PBS), pH 8.0, TCR was purified using W4F.5B Ab-affinity chromatography (2) and concentrated to 1 mg/ml. S2 cells expressing soluble HLA-DR1 were a gift from Dennis Zaller (Merck Research Laboratories, Rahway, NJ). The HLA-DR1 heterodimer was produced as previously described (45) and loaded with the peptide consisting of positions 308 to 319 of FluHA ($FluHA_{308-319}$; Chiron Mimotopes, Sydney, Australia).

Biacore system analysis. The binding of superantigens to human Vβ8.1 TCR and HLA-DR1 was measured by surface plasmon resonance using a Biacore 2000 system (Biacore AB, Uppsala, Sweden). SMEZ-2 wild-type and mutants were immobilized on the dextran matrix of CM5 sensor chips with an amine coupling kit (Biacore). All superantigens were coupled in 10 mM sodium acetate buffer; optimal preconcentrations were 10 μg/ml of SMEZ-2 wild type at pH 4.5, 15 μg/ml of M1 and 10 μg/ml of DM at pH 4.0, and 20 μg/ml of M2 at pH 5.0. Buffer consisting of HEPES (10 mM), 0.15 M NaCl, and 0.005% (vol/vol) P20 surfactant (HBS-P; degassed and filtered) was used as a continuous running buffer for all binding studies. The Vβ8/α1 TCR and HLA-DR1 (loaded with $FluHA_{308-319}$ peptide) were diluted in running buffer. Binding was monitored at 25°C for 3 min at a constant flow rate of 20 μl/min. The activity of the sensor surface was analyzed using a triplicate injection of purified Vβ8/α1 TCR at 1 mg/ml. Subsequent binding experiments used a 2-fold dilution series of TCR from 500 μg/ml to 7.8 μg/ml. Binding of HLA-DR1 to SMEZ-2 wild type and mutants was performed at 10 and 1 μM in running buffer. Sensor chip surfaces were regenerated using a triplicate injection pulse of 10 mM HCl for TCR and 50 mM H_3PO_4 for DR1. Sensorgram data were analyzed with BIAevaluation software, version 3.1.1 (Biacore): during binding studies, inline reference subtraction, which removed background/bulk shift responses, producing binding curves of the response difference between reference and ligand flow cells, was used. Overlay plots were produced by alignment of time and response axes for the curves.

Proteins and peptides. Ovalbumin (OVA) and a peptide consisting of OVA from positions 323 to 339 ($OVA_{323-339}$) was purchased from Sigma-Aldrich. The $OVA_{323-339}$ peptide (36, 37) was custom synthesized to

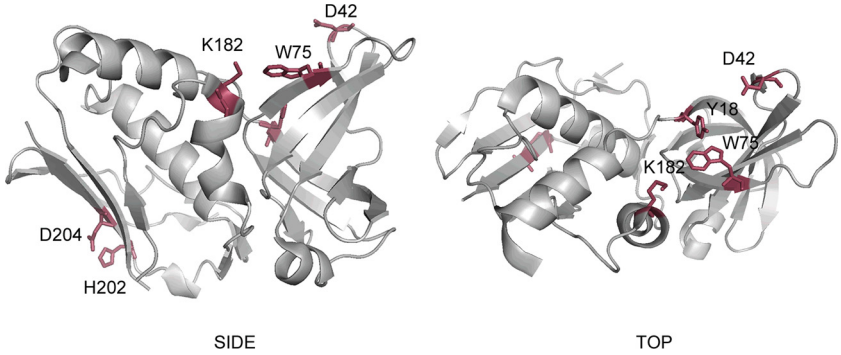

FIG 1 Location of residues involved in TCR binding (Y18, D42, W75, K182) and MHC class II binding (D202, H204). Placement of the antigen coupling site (D42C) interferes with TCR binding while leaving the MHC class II binding site free.

>95% purity and included a cysteine at the N terminus to permit coupling of the peptide to the M1 carrier. Proteins were labeled using fluorescein isothiocyanate (FITC) *N*-hydroxysuccinimide ester (Sigma-Aldrich) or a Cy5 bisfunctional reactive dye according to the manufacturer's instructions (Amersham Pharmacia, United Kingdom).

Mice. Female C57BL/6 and BALB/c mice 6 to 8 weeks old were purchased from the VJU, University of Auckland, Auckland, New Zealand. Transgenic mice that lack endogenous MHC class II (IAE^-) and express human CD4 (hCD4) and either human DR4-DQ8 (7) or DR3-DQ2 (8) (here shortened to DR4-DQ8 and DR3-DQ2, respectively) were kindly supplied by James McCluskey, University of Melbourne, Melbourne, Australia. Immunization experiments with transgenic mice and controls used age-matched male and female mice aged ~4 months. C57BL/6 control mice for the transgenic studies were from the VJU or generously provided by The Malaghan Institute, Wellington, New Zealand. Animals were housed and cared for under specific-pathogen-free conditions in accordance with the Animal Welfare Act (1999) and institutional guidelines provided by the University of Auckland Animal Ethics Committee, which reviewed and approved these experiments.

For vaccination studies, coupled protein or peptide antigens were diluted in sterile PBS, emulsified 1:1 in incomplete Freund's adjuvant (IFA; Sigma), and delivered subcutaneously into the nape of the neck. Blood was sampled from the tail vein at regular intervals, collected in Microvette 500 serum-gel tubes (Sarstedt, Germany), processed, and stored at −20°C.

Cell culture. Human peripheral blood mononuclear cells (PBMCs) and murine splenocytes were prepared as outlined elsewhere (44). For proliferation assays, 1×10^5 PBMCs and 2×10^5 splenocytes per well were cultured in serial dilutions of recombinant superantigens, and proliferation was quantified by adding 0.25 μCi [^{3}H]thymidine (Amersham) per well on day 3. Approximately 16 h later, cells were harvested onto glass filter mats and [^{3}H]thymidine uptake was quantified using a beta scintillation counter (all from Wallac OY, Finland).

The acute monocytic leukemia cell line THP-1 (ATCC) was maintained as per ATCC recommendations and activated by combining 0.5×10^6 cells/ml and 200 U/ml gamma interferon (IFN-γ) for 2 days to upregulate MHC class II expression. Cells were incubated with 1 μM FITC-conjugated protein for 20 min at 4°C to measure MHC class II binding by flow cytometry. Dendritic cells were derived from the bone marrow of C57BL/6 mice as described by Inaba et al. (22), and semiadherent cells were used on day 6. All cell culture materials were purchased from Invitrogen, New Zealand.

Microscopy. IFN-γ-activated THP-1 cells were stained with 1 μM M1-FITC for 20 min at 4°C, washed in PBS, and incubated at 37°C for 0, 30, or 120 min in culture medium. Cells were then washed in PBS, fixed in 4% paraformaldehyde (5 min, 37°C), and mounted onto poly-L-lysine-coated glass slides. Images were captured on a Nikon E600 fluorescence microscope. Dendritic cells were triple stained in PBS–0.5% bovine serum albumin (BSA)–5% normal rabbit serum–5% normal mouse serum with anti-mouse MHC class II (I-A/I-E), N418-FITC, and M1-Cy5. Cells were washed twice in PBS and incubated for 10 min at 4°C with streptavidin-Cy3 (Amersham Pharmacia, United Kingdom). Dendritic cells were then either left on ice or incubated at 37°C for 0.5 h prior to fixation with 4% paraformaldehyde. Fixed cells were mounted on poly-L-lysine-coated glass slides with fluorescent mounting medium (Dako, Germany). Images were captured on a Leica TC SP2 confocal microscope.

***In vivo* localization of iodinated superantigens.** Twenty micrograms of recombinant superantigens was radioiodinated by the chloramine T method as previously described (27). Excess ^{125}I was removed from labeled superantigen by size exclusion chromatography using Sephadex G25 columns. ^{125}I-labeled superantigen was mixed with cold superantigen to a final concentration of 10 μCi/ml. Then, 1 μCi/mouse, corresponding to 10 μg or 0.4 nmol total superantigen, was injected subcutaneously into C57BL/6 mice. Lymph nodes, spleen, lung, liver, and kidney were collected after 24 h and measured in a Cobra II autogamma counter, and counts for organs were normalized with respect to weight.

Cytokine assays. Human PBMCs (1×10^5) from five healthy volunteers were stimulated with 100-ng/ml recombinant superantigen, and supernatants were harvested after 72 h. Cytokine levels were determined by a human cytokine LINCOplex kit (Linco Research). Evaluation of the data was performed by a 5-parameter logistic curve-fitting method for calculating the cytokine concentration using the Luminex software 100 IS.

Mice were given a 10-μg dose of SMEZ-2 wild type, SMEZ-2 M1, or PBS via the intraperitoneal route to determine whether the SMEZ-2 M1 carrier elicited a proinflammatory cytokine response *in vivo*. After 3 h, blood was sampled from the tail vein and processed for serum. Serum was diluted 1/3 for assay with a mouse inflammation kit (BD Biosciences), and cytokine concentrations were determined by a 4-parameter logistic curve-fitting method using FCAP Array software (BD Biosciences).

Cell-associated interleukin-4 (IL-4) and IFN-γ production was measured with an enzyme-linked immunosorbent spot (ELISPOT) assay set (BD Biosciences) as per the manufacturer's instructions. Splenocytes were cultured in triplicate at 1×10^5 and 2×10^5 cells/well for 16 h in the presence of 100 μg/ml OVA. Control wells were set up in parallel and stimulated with 0.5 μg/ml concanavalin A (Sigma) or medium alone to confirm that the number of functional cells per well was equivalent across all individual mice and to establish background numbers of cytokine-secreting cells. The number of spot-forming cells (SFCs) per well was determined manually by light microscopy (×20 magnification). The medium control values were subtracted from OVA-stimulated cell values and used to calculate the number of SFCs per 10^6 splenocytes.

Flow cytometry. Cells were counted, suspended at 10^6 cells/tube, and labeled for 20 min on ice with antibodies directly conjugated to cell surface markers (BD Biosciences). Labeled cells were washed and resuspended in PBS–2% fetal bovine serum–0.02% NaN_3 supplemented with 0.5 μg/ml propidium iodide (Invitrogen) to enable selection of viable cells. Cells were analyzed with a FACScan or LSR II flow cytometer equipped with CellQuest or FACSDiva software (BD Biosciences).

Conjugation of peptide and proteins to carrier. Recombinant SMEZ-2 M1 and DM (0.2 mM) were reduced for 1 h at room temperature (RT) with 0.1 M dithiothreitol (DTT) and buffer exchanged into 0.1 M Tris, pH 8.0, immediately prior to conjugation to remove DTT. Synthetic peptide was solubilized in 0.1% acetic acid and conjugated to purified SMEZ-2 M1 or DM at a 10:1 molar ratio by overnight incubation with 200 mM Tris HCl, pH 8, 2 μM $CuSO_4$ to promote disulfide bond formation between the exposed cysteine residue on the M1 carrier and the cysteine present on the N terminus of the $OVA_{323-339}$ peptide. Free peptide was removed by buffer exchange through a 5,000-molecular-weight-cutoff Vivaspin concentrator (Vivascience, Germany). Conjugated peptide was concentrated by buffer exchange into 0.1 M Tris, pH 8.0, filter sterilized (0.22 μM), and stored at 4°C. Peptides remained stably coupled for some months after conjugation.

Peptide conjugation was confirmed by 17% SDS-PAGE (24) and Coomassie blue staining. M1 and M1–$OVA_{323-339}$ conjugates were transferred onto a nitrocellulose membrane (Pall Life Sciences) (42) and probed with serum from OVA-immunized mice diluted 1:500. The membrane was stripped and reprobed with a mouse anti-M1 monoclonal antibody at 0.2 μg/ml. Both primary antibodies were detected using anti-mouse IgG-horseradish peroxidase (HRP; Jackson ImmunoResearch) at 0.08 μg/ml and enhanced chemiluminescence Western blotting substrate (Pierce). Images were acquired using a FujiFilm LAS-3000 image analyzer. M1–$OVA_{323-339}$ conjugates were run through a Superdex 200 5/150 GL (GE Healthcare) analytical column under reducing (1 mM DTT) and nonreducing conditions. A_{280} data were collected using fast-performance liquid chromatography (FPLC).

OVA was stably cross-linked to SMEZ-2 M1 or DM with sulfo-succinimidyl-4-(*N*-maleimidomethyl)cyclohexane-1-carboxylate (SMCC) cross-linker (no. 22322; Pierce Chemicals). M1 and DM proteins (0.2 mM) were reduced with DTT as described above, and DTT was removed on a G10

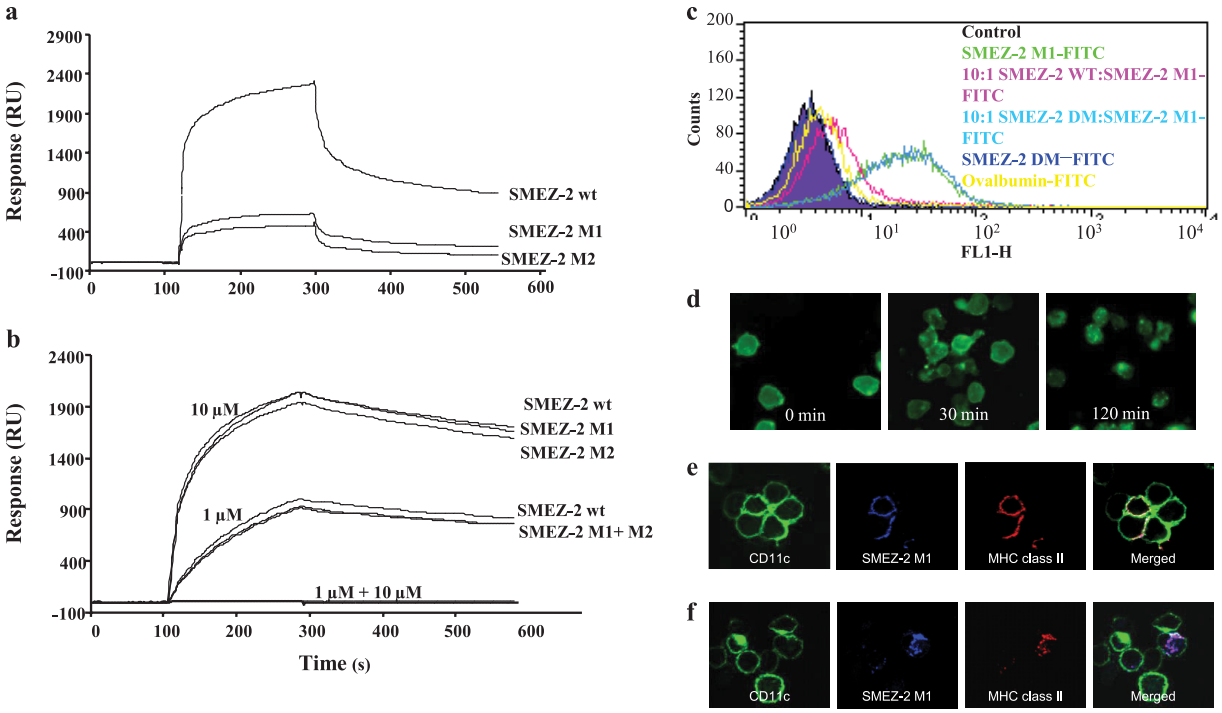

FIG 2 Superantigen mutants no longer bind to the TCR but retain specificity for MHC class II and are internalized into antigen-presenting cells. (a and b) SMEZ-2 wild type (wt), M1, M2, and DM were immobilized on a dextran chip of a Biacore biosensor. As analytes, 1 mg/ml soluble Vβ8/α1 TCR (a) and 1 μM and 10 μM HLA-DR1 (b) were injected at a flow rate of 20 μl/min. Curves represent triplicate injections with binding in relative response units (RUs), with the background binding to a plain dextran surface subtracted. (c) FACS analysis of SMEZ-2 binding to THP-1 cells. FITC (1 μM)-conjugated protein was incubated with 1×10^5 THP-1 cells for 20 min at 4°C. Competition with unlabeled superantigen occurred at a 10:1 molar ratio where indicated. Cells were washed and analyzed by flow cytometry. (d) SMEZ-2 M1 binding of THP-1 cells imaged on a Nikon E600 fluorescence microscope. THP-1 cells were incubated with 1 μM FITC-conjugated SMEZ-2 M1 for 20 min at 4°C, before washing and incubating at 37°C in medium for 0, 30, or 120 min. (e and f) Murine BMDCs were incubated for 10 min at 4°C with fluorescence-labeled anti-CD11c, SMEZ-2 M1, and anti-MHC class II. Dendritic cells were washed and analyzed by confocal microscopy before (e) or after (f) a further incubation for 30 min at 37°C.

desalting column (Bio-Rad, Australia). Sulfo-SMCC was combined with OVA at a molar ratio of 10:1 at RT for 1 h. Free sulfo-SMCC was removed using a G10 desalting column, and the derivatized OVA protein was immediately incubated overnight with the reduced SMEZ-2 M1 and DM at a molar ratio of 1:1. The cross-linked proteins were separated from uncoupled protein by size-exclusion FPLC (Superdex 200 10/30 GL column; GE Pharmaceuticals). High-molecular-weight fractions were combined and concentrated to ~2 mg/ml (20 nM) by ultrafiltration. Endotoxin was removed from the M1-OVA and DM-OVA conjugates by Triton X-114 extraction (28) and confirmed by *Limulus* amoebocyte lysate assay. The conjugates were sterilized through a 0.22-μm-pore-size filter and stored in aliquots at 4°C.

Assessment of specific serum Ab responses. Maxisorp microtiter plates (Nunc, Denmark) were coated with 0.5 μg or 0.25 μg per well protein or peptide in PBS. The plates were blocked with 2% BSA in PBS and washed with 0.05% Tween 20 in PBS, and bound antibody was detected using HRP-conjugated anti-mouse IgG, IgG1 (Serotec, United Kingdom), or IgG2c (Jackson ImmunoResearch, PA) and *o*-phenylenediamine substrate. Serial 2-fold dilutions of 0.1 μg per well mouse anti-OVA IgG1 Ab (OVA-14; Sigma-Aldrich) or mouse anti-M1 IgG1 Ab were used as a standard in some assays. Plates were read at 490 nm, and a 4-parameter fit of the standard curve was produced with KC4 software (Bio-Tek Instruments, Inc.). Endpoint titers were used to determine anti-OVA IgG Ab levels in transgenic and control mice, starting at a 1/100 dilution. The endpoint was $(2 \times A_{490}) + (2$ standard deviations [SDs]) of a baseline serum sample.

Statistics. *P* values were calculated using Prism (version 5.02) software (GraphPad Software, Inc., CA). The tests applied are detailed in the figure legends. A *P* value of 0.05 was considered to be statistically significant.

RESULTS

TCR-defective SMEZ-2 retains MHC class II binding. Surface plasmon resonance was used to compare the direct binding of SMEZ-2 and mutants M1, M2, and DM to soluble forms of human Vβ8/Vα1.2 TCR and HLA-DR1 FluHA$_{308\text{-}319}$. SMEZ-2, M1, M2, and DM were coupled to separate dextran sensor chips at 2,138, 2,579, 3,535, and 2,232 relative response units (RU), respectively. Soluble human Vβ8 (hVβ8)/Vα1.2 TCR binding to immobilized SMEZ-2 was characterized by fast association and slow dissociation, consistent with other studies of direct binding of soluble TCR to superantigens (26). For simplicity, only the response to the highest TCR concentration (1 mg/ml) is shown (Fig. 2a). At this concentration, soluble Vβ8/Vα1.2 TCR bound to SMEZ-2 with 2,000 RU, while M1 and M2 bound with approximately 400 RU. At 250 μg/ml of TCR, binding to M1 or M2 was undetectable (data not shown), while SMEZ-2 bound at 400 RU. No difference was observed for wild-type SMEZ-2, M1, or M2 binding to DR1–FluHA$_{308\text{-}319}$ at either 1 or 10 μM (Fig. 2b). Binding of MHC class II to the DM mutant was undetectable. Addition of 1 μM EDTA to the analyte destroyed binding of soluble DR1–FluHA$_{308\text{-}319}$ to SMEZ-2 and mutants, confirming that binding was mediated by zinc (data not shown). These studies verified the intended mutations of M1 and the independence of TCR and MHC class II binding sites on the molecule. The M1 and M2 TCR-negative mutants of

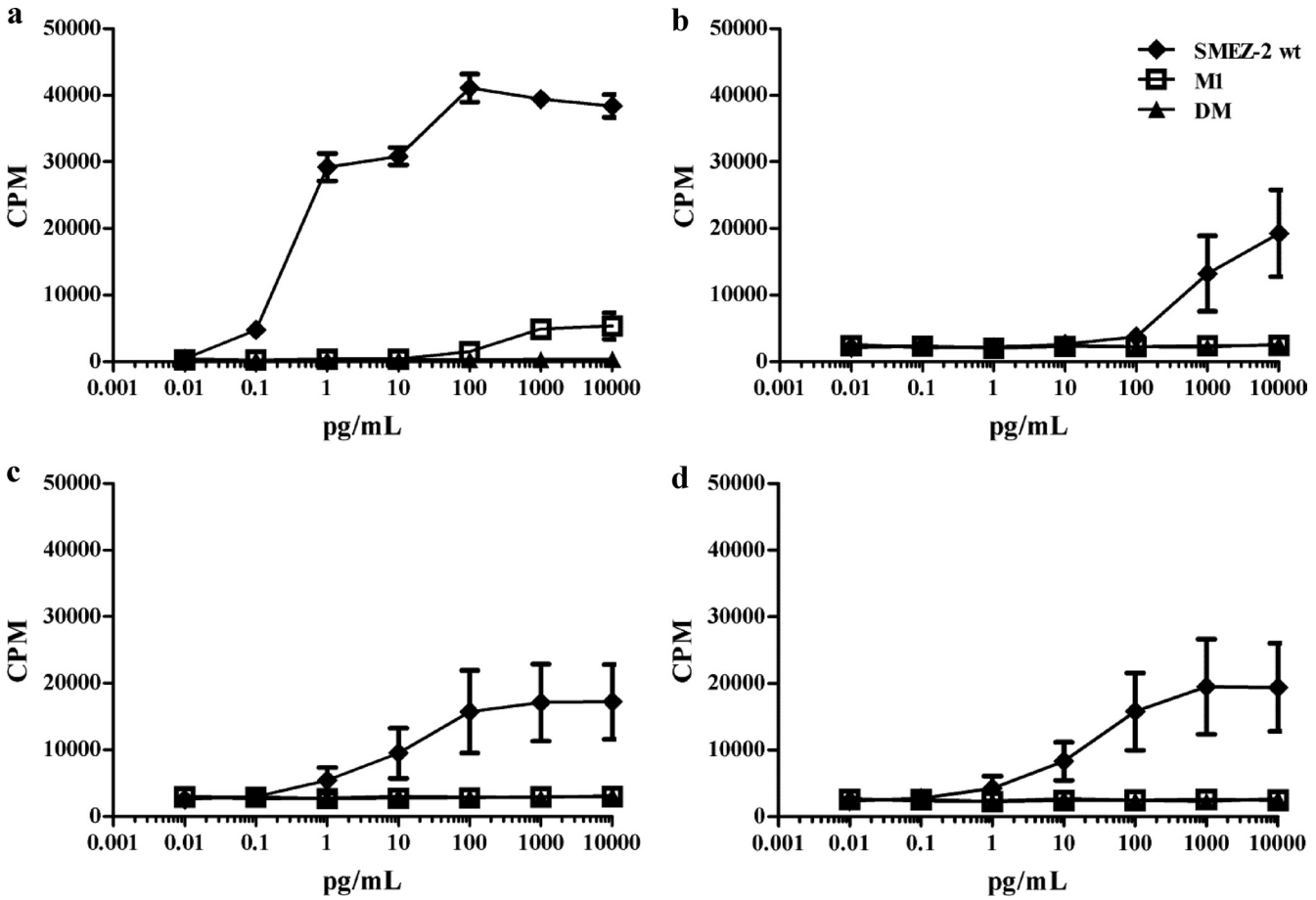

FIG 3 SMEZ-2 M1 does not stimulate T cell proliferation from human or murine immune cells. Human PBMCs (a), murine C57BL/6 (b), or humanized DR3-DQ2 (c) or DR4-DQ8 (d) transgenic splenocytes were cultured with graded doses of SMEZ-2 wild type (wt), M1, and DM for 3 days, and proliferation was quantified by uptake of tritiated thymidine over the final 16 h of the culture period. Murine data are the mean ± SD from 10 individual mice per figure combined from 5 independent experiments. Results for human PBMCs (mean ± SD from triplicate wells) from a single healthy donor are shown as a point of comparison.

SMEZ-2 showed comparable specificities in this assay, and the M1 protein, which had 3 mutated TCR-binding residues, was selected for further investigation.

SMEZ-2 M1 binds to MHC class II and is internalized. M1 was examined for its ability to bind to IFN-γ-activated MHC class II-positive (MHC class II^+) THP-1 cells. M1-FITC bound to IFN-γ-treated THP-1 cells and was effectively blocked by an excess of the parental SMEZ-2 but not by DM (Fig. 2c). A low level of binding to THP-1 cells was also observed with the control protein OVA (Fig. 2c). Fluorescence microscopy allowed direct visualization of THP-1 cells surface stained with M1-FITC at time zero, followed by internalization after incubation at 37°C for 30 min (Fig. 2d). By 2 h, all M1-FITC was located within intracellular vesicles (Fig. 2d). A similar result was observed with murine C57BL/6 bone marrow-derived dendritic cells (BMDCs) (Fig. 2e). Triple-color staining of M1-FITC, CD11c, and MHC class II showed that M1 and MHC class II were internalized into the same intracellular vesicle in BMDCs and were superimposed within 30 min. This confirmed that M1 initiated and remained bound to MHC class II during internalization into what is presumed to be the MHC class II compartment (Fig. 2f).

SMEZ-2 M1 does not stimulate T cell proliferation. SMEZ-2 is the most potent superantigenic mitogen toward human T cells, with a calculated concentration generating a half-maximal proliferative response of 0.2 pg/ml (Fig. 3a) (33). M1 was 10^5-fold less active, with only minimal proliferation detected at the highest concentration of 10 ng/ml (Fig. 3a), while the DM mutant lacking MHC class II binding displayed no proliferative response to human PBMCs at any concentration (Fig. 3a). SMEZ-2 was 10^4-fold less potent toward C57BL/6 murine splenocytes, requiring 1 ng/ml to generate a half-maximal proliferative response (Fig. 3b). This reflected a reduced affinity for murine MHC class II that was substantially corrected in splenocytes expressing either DR3-DQ2 (Fig. 3c) or DR4-DQ8 (Fig. 3d). These cells required 10 pg/ml of SMEZ-2 to generate half-maximal proliferation, although the absolute cell proliferation was substantially less than that in human splenocytes, perhaps reflecting a lower frequency of SMEZ-2-responsive T cells (Fig. 3b). M1 and DM displayed no measureable proliferative activity toward splenocytes from C57BL/6 or C57BL/6 human class II transgenic mice (Fig. 3b to d).

SMEZ-2 M1 does not stimulate cytokine responses or expansion of T cells. SMEZ-2 elicits a substantial *in vitro* cytokine response from human PBMCs, stimulating very high levels (>2,000 pg/ml) of IL-2, IL-6, and IFN-γ and moderate levels of IL-10 and

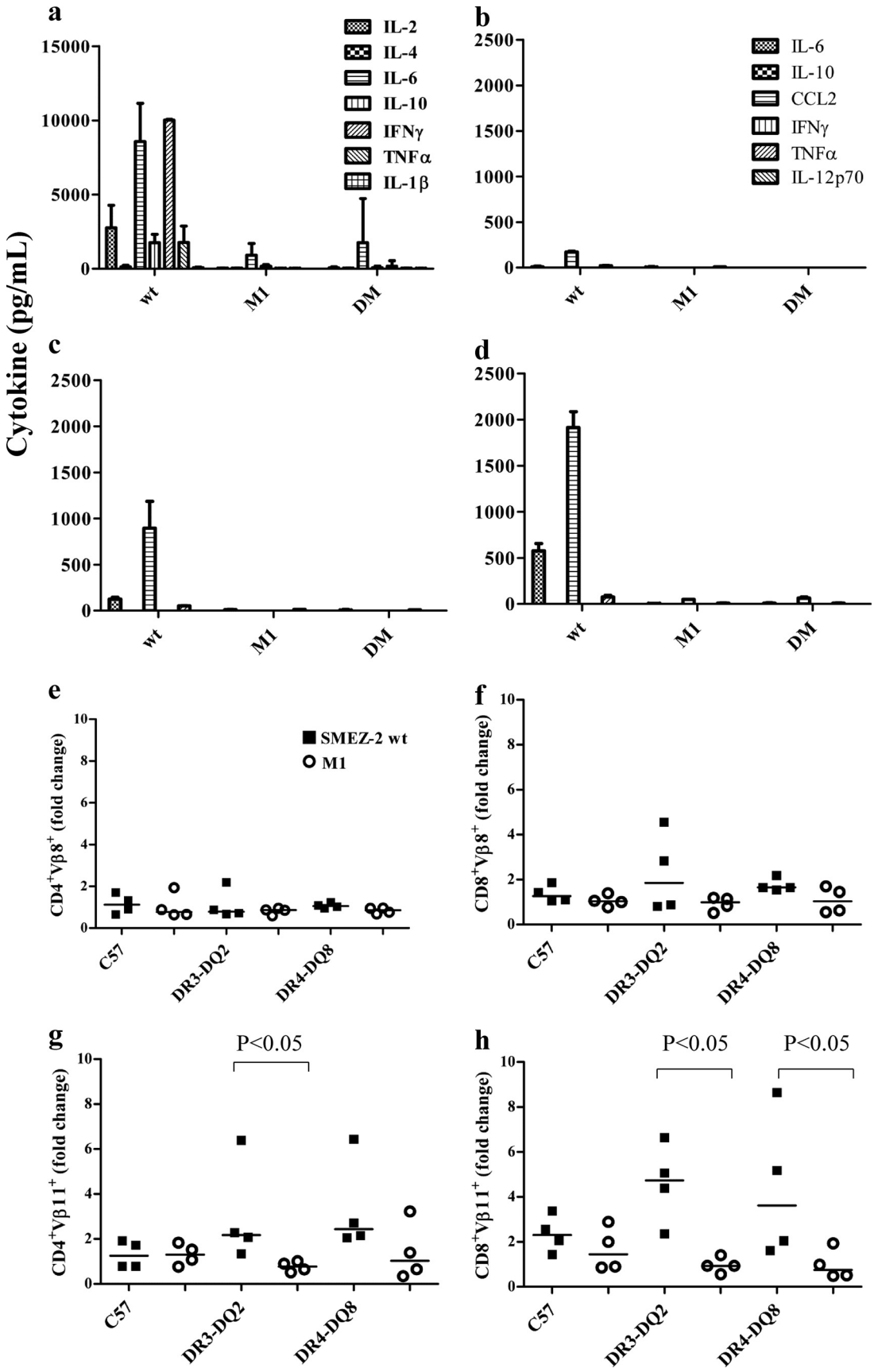
a
b
c
d
e
f
g
h
Cytokine (pg/mL)
IL-2
IL-4
IL-6
IL-10
IFNγ
TNFα
IL-1β
IL-12p70
CCL2
wt
M1
DM
SMEZ-2 wt
M1
CD4+Vβ8+ (fold change)
CD8+Vβ8+ (fold change)
CD4+Vβ11+ (fold change)
CD8+Vβ11+ (fold change)
C57
DR3-DQ2
DR4-DQ8
P<0.05
P<0.05
P<0.05

tumor necrosis factor alpha (TNF-α) (Fig. 4a). In contrast, PBMCs stimulated with M1 produced only background cytokine levels, confirming that TCR engagement was essential for cytokine production.

In vivo cytokine responses to SMEZ-2 were elevated >2-fold (TNF-α), >4-fold (chemokine [C-C motif] ligand 2 [CCL2]), and >10-fold (IL-6) in DR3-DQ2 and DR4-DQ8 transgenic mice relative to the parental C57BL/6 mice, confirming the importance of human MHC class II and human CD4 in maximal cytokine production (Fig. 4b to d). The highest level of all three cytokines was detected in the serum from DR4-DQ8 mice treated with SMEZ-2 (Fig. 4d). Exposure of these mice to equivalent amounts of M1 did not elicit any significant cytokine response (Fig. 4b to d).

SMEZ-2 activates murine T cells expressing the murine Vβ11 (mVβ11) TCR but not the mVβ8 TCR (35, 44). The proportion of Vβ11 TCR-positive (TCR$^+$) CD4$^+$ and CD8$^+$ T cells was thus increased 2- to 4-fold in the DR3-DQ2 and DR4-DQ8 mice 3 days after exposure to SMEZ-2, while the frequency of Vβ8 TCR$^+$ T cells remained unchanged (Fig. 4e to h). In comparison, transgenic mice treated with M1 showed no detectable increase in Vβ11 TCR$^+$ CD4 or CD8 T cells. Together, these data confirmed that M1 was inactive as a T cell mitogen in human MHC class II/CD4 transgenic mice.

SMEZ-2 wild type and M1 but not DM are transported to the lymph node. Staphylococcal enterotoxins A and B are detectable from as early as 6 h in the lymph nodes and spleen after intraperitoneal injection of mice, with an increase of total DC numbers and an increase of costimulatory molecules on DCs in the T cell areas (31, 47). To follow the *in vivo* trafficking of SMEZ-2 and its mutants, SMEZ-2, M1, M2, and DM were radioiodinated and injected subcutaneously into C57BL/6 mice. The tissue distribution of SMEZ-2 was determined by removing organs 24 h after injection, counting in a gamma counter, and then adjusting for organ weight. Figure 5a shows that SMEZ-2 concentrated in the draining lymph node with a 4- to 8-fold higher specific level than SMEZ-2 concentrated in the spleen, kidney, lung, or liver. M1 and M2 also concentrated into the draining lymph nodes, although the ratios compared to those for the other organs were reduced between 2- and 5-fold (Fig. 5b and c). DM was evenly distributed throughout all tissues, indicating that MHC class II binding was essential for the concentration of M1 in lymphoid tissue (Fig. 5d). The substantially higher ratio of wild-type SMEZ-2 than M1 and M2 in draining lymph nodes suggested that T cell activation also contributed to lymphoid entrapment. These data indicate that M1 conjugates injected into mice are likely to concentrate antigen to secondary lymph nodes.

Conjugation of proteins/peptides to SMEZ-2 M1. Synthetic peptides were conjugated to M1 or DM via the cysteine residue at position D42C using a simple reversible disulfide oxidation that provided a fixed superantigen/peptide molar ratio of 1:1. Peptide conjugation was confirmed by 17% SDS-PAGE, with conjugate preparations running at a slightly higher molecular mass than monomeric M1 (Fig. 6a, lanes A1 and A2). Minimal quantities of dimeric M1-DM protein (~50 kDa) were evident, suggesting a high conjugation efficiency. When peptide was added at a 10-fold molar excess, the reaction was routinely >90% efficient.

Due to the small difference in molecular mass (~2 kDa) between the M1 and M1–OVA$_{323\text{-}339}$ proteins, conjugation was verified by Western blotting. Samples were transferred to a nitrocellulose membrane, probed with anti-OVA antiserum (Fig. 6a, lanes B1 and B2), and then stripped and reprobed with M1 monoclonal antibody (Fig. 6a, lanes C1 and C2). Bound antibody was detected with anti-mouse IgG-HRP to confirm that OVA$_{323\text{-}339}$ peptide was incorporated into the M1–OVA$_{323\text{-}339}$ conjugate. Additionally, conjugates were excised from an SDS-polyacrylamide gel and processed for liquid chromatography-mass spectrometry, and the most abundant sequences were found to match published sequences for SMEZ-2 and the sequence in an in-house database containing the modified OVA$_{323\text{-}339}$ peptide sequence ($P < 0.05$; data not shown). M1–OVA$_{323\text{-}339}$ preparations were also run through an analytical sizing column, and the A_{280} was measured to demonstrate that the nonreduced sample comprised a single dominant peak (M1–OVA$_{323\text{-}339}$), while the reduced sample had two peaks representing free M1 protein and an OVA$_{323\text{-}339}$ peptide peak (Fig. 6b).

The chemical cross-linker sulfo-SMCC was used to couple OVA protein, and this process was approximately 30 to 50% efficient and produced conjugates containing M1-OVA at ratios of 1:1 and 2:1 with an average molecular mass of approximately 70 kDa (Fig. 6c).

SMEZ-2 M1 enhances Ab responses to conjugated peptide. Initial vaccination studies were performed in BALB/c mice using OVA protein coupled to the M1 carrier and demonstrated that a single injection with 10 μg M1-OVA in IFA produced significantly enhanced anti-OVA IgG responses and required chemical coupling of M1 to OVA (data not shown). Later studies indicated that the carrier effect of M1 was more significant in C57BL/6 mice, a strain that produces a very weak antibody response to OVA in IFA.

Further vaccination studies were performed in C57BL/6 mice, testing the ability of M1 to enhance IgG production to a B cell peptide epitope, OVA$_{323\text{-}339}$. A single vaccination with M1–OVA$_{323\text{-}339}$ in IFA produced significantly higher specific antibody responses after 25 days (median = 100 μg/ml) and 42 days (median = 90 μg/ml) (Fig. 7a) compared to those after 42 days in mice immunized with peptide alone in IFA (median = 0.5 μg/ml). Importantly, the absolute amount of coupled peptide was 3-fold less (~0.35 μg) in mice receiving the conjugate relative to the control animals (1 μg), showing that M1 induced higher responses with less antigen. C57BL/6 mice vaccinated with the nontargeting control preparation DM–OVA$_{323\text{-}339}$ in IFA developed

FIG 4 (a to h) SMEZ-2 M1 fails to stimulate cytokine production or *in vivo* expansion of Vβ11$^+$ T cells. (a) Human PBMCs were incubated with 100 ng/ml SMEZ-2 wild type (wt), 100 ng/ml M1, or no antigen. The cytokine response was quantified in culture supernatants after 72 h at 37°C. Results are shown as the mean concentration ± SD of five donors. (b to d) The serum cytokine response was measured 3 h after intraperitoneal injection with 10 μg SMEZ-2, M1, or PBS in age-matched wild-type C57BL/6 (b), DR3-DQ2 (c), and DR4-DQ8 (d) mice. Data are presented as the mean ± SD for 2 mice per treatment per strain; a total of 18 mice were used per study. These data are representative of two independent experiments. (e to h) Three days after injection of 10 μg SMEZ-2, SMEZ-2 M1, or PBS, T cell populations were enumerated by combining data from whole-spleen-cell counts with flow cytometric analysis: CD4$^+$ Vβ8$^+$ (e), CD8$^+$ Vβ8$^+$ (f), CD4$^+$ Vβ11$^+$ (g), and CD8$^+$ Vβ11$^+$ (h). The fold change in T cell numbers was determined relative to the PBS control group. Data were combined from two independent experiments ($n = 4$ per treatment group; $n = 36$ mice in total). Each point represents a single mouse, and the horizontal bar is the median value. *P* values were calculated using a one-tailed Mann-Whitney test.

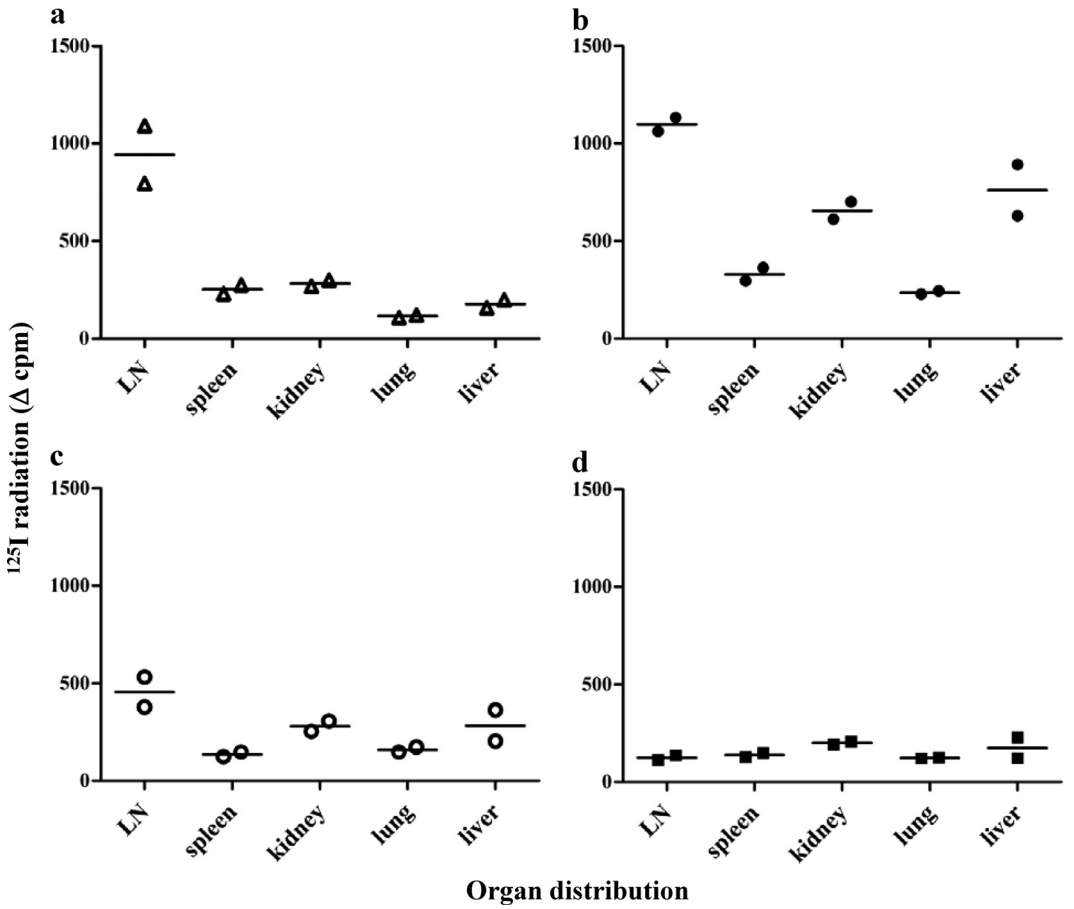

FIG 5 *In vivo* trafficking of superantigens. C57BL/6 mice ($n = 2$) were injected subcutaneously with 0.4 nmol ^{125}I-labeled superantigen: SMEZ-2 wild type (a), SMEZ-2 M1 (b), SMEZ-2 M2 (c) and SMEZ-2 DM (d). Twenty-four hours later, mice were sacrificed, lymph nodes (LN), spleen, kidney, lung, and liver were collected, and the ^{125}I incorporation was measured in a gamma counter. Data are normalized with respect to the weight of the organs; each point represents a single mouse, and the horizontal line is the median value. Data are representative of two experiments ($n = 8$ mice per experiment).

no detectable response, confirming the requirement for MHC class II binding.

Anti-M1 Ab responses do not reduce the activity of the M1 carrier. The M1 protein by itself is immunogenic and stimulates a strong antibody response in mice (Fig. 7b) and humans (34). To determine whether preexisting anti-M1 antibodies altered the M1 carrier effect by blocking binding to MHC class II, C57BL/6 mice were first immunized with M1 or PBS and then later vaccinated with M1-OVA conjugate. Comparable levels of anti-OVA IgG developed in both groups of mice, all of which had similar levels of preexisting anti-M1 antibody (Fig. 7b). However, the range of anti-OVA IgG in the M1-seroconverted group was substantially larger ($n = 7$, range = 100 to 40,000 μg/ml) than that in the sham-preimmunized group ($n = 7$, range = 800 to 2,000 μg/ml). This indicated that anti-M1 antibody did not prevent the M1 carrier effect and in some animals actually dramatically enhanced the response.

SMEZ-2 M1 enhances Ab responses in DR3-DQ2 and DR4-DQ8 transgenic mice. Superantigens have higher affinity toward human than mouse MHC class II. Vaccination studies were therefore performed in C57BL/6 mice transgenic for human CD4 and either DR3-DQ2 or DR4-DQ8, and the results were compared to those for parental C57BL/6 mice. Mice were immunized subcutaneously once with 10 μg of antigen in IFA, and circulating specific serum anti-OVA IgG was measured at regular intervals. All mice vaccinated with M1-OVA rapidly developed high levels of anti-OVA IgG as early as 2 weeks postvaccination. At week 2, C57BL/6 mice displayed a median anti-OVA IgG endpoint titer of 1,000 (Fig. 8a), DR3-DQ2 mice displayed an endpoint titer of 10,000 (Fig. 8b), and DR4-DQ8 mice displayed an endpoint titer of 80,000 (Fig. 8c). By week 5 these levels had increased 5-fold (DR4-DQ8 and DR3-DQ2; Fig. 8b and c) and 40-fold (C57BL/6; Fig. 8a). The DR3-DQ2 mice ultimately displayed the highest median endpoint titer of 200,000 (Fig. 8c). In contrast, vaccination with OVA alone was less effective, with 3/5 C57BL/6, 1/5 DR3-DQ2, and 3/5 DR4-DQ8 mice failing to develop any detectable anti-OVA IgG response by week 5 (Fig. 8a to c). A comparative assessment of specific IgG1 and IgG2c subtype (30) responses to M1-OVA in the vaccinated animals showed that the subtype was strongly biased toward IgG1 (Fig. 8d), suggesting that M1 conjugation promotes a strong Th2-type response (38).

The M1 carrier stimulates enhanced *in vitro* but not *in vivo* cellular responses. BALB/c mice were immunized subcutaneously with 10 μg OVA in IFA (weeks 0 and 3) to generate OVA responder cells, which were then tested for proliferation responses to OVA protein or the equivalent quantity of OVA

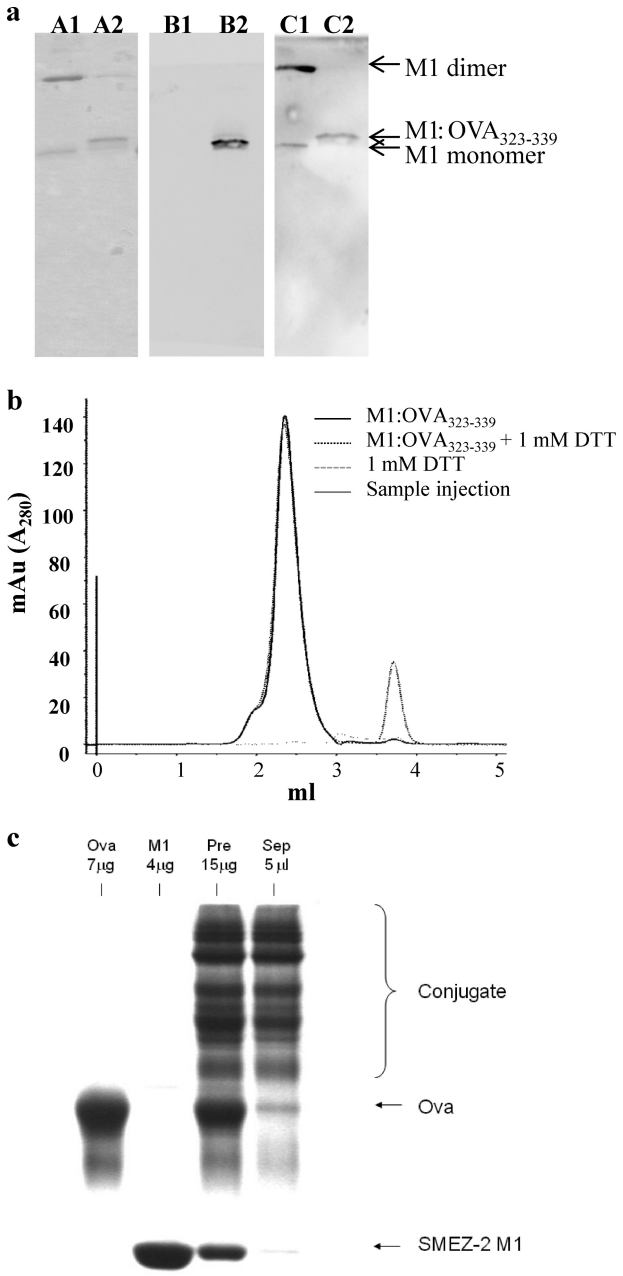

FIG 6 $OVA_{323-339}$ peptide and OVA protein can be chemically conjugated to the M1 carrier. (a) Conjugation efficiency was checked by 17% SDS-PAGE in nonreducing sample buffer, and protein was detected using Coomassie blue (lanes A). The identity and colocalization of the $OVA_{323-339}$ (lanes B) and M1 (lanes C) were confirmed by Western blotting. Lanes A1, B1, and C1, M1; lanes A2, B2, and C2, M1–$OVA_{323-339}$. (b) To further verify chemical coupling of peptide to conjugate, samples were run through an analytical sizing column in the presence or absence of 1 mM DTT, and the number of peaks was assessed at A_{280}. mAu, milli-absorbance units. (c) Representative fractions of conjugated protein before, during, and at the end of purification by size exclusion were run using 12% SDS-PAGE in nonreducing sample buffer and stained with Coomassie blue. OVA-M1 protein conjugates are indicated by a bracket. Lanes from left to right: OVA, M1, conjugated but unseparated M1-OVA (Pre), and conjugated M1-OVA after purification by size exclusion (Sep).

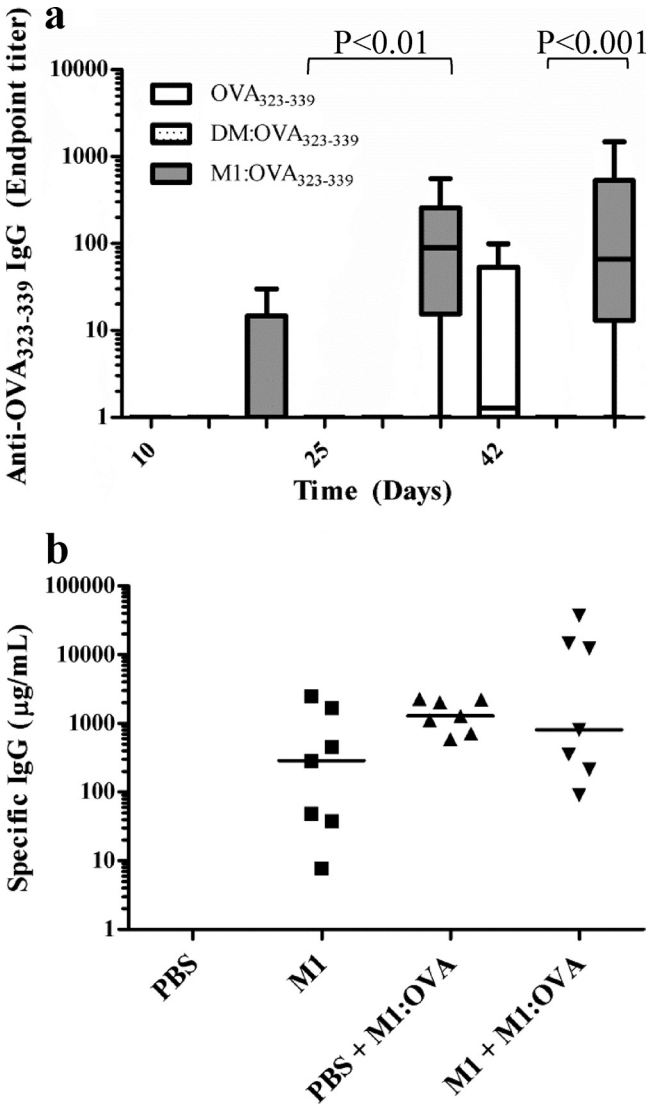

FIG 7 The M1 carrier enhances antibody responses to coupled peptide and is effective in the presence of specific anti-M1 antibodies. (a) C57BL/6 mice were vaccinated once with M1–$OVA_{323-339}$, DM–$OVA_{323-339}$, or peptide alone, all emulsified in IFA. IgG responses are shown as whisker plots showing the minimum to maximum range of data points and the median value. Data are representative of two independent experiments, each containing 5 mice per group and 15 mice in total. (b) BALB/c mice were immunized with 10 μg M1 or PBS in IFA, followed by vaccination with 10 μg M1-OVA in IFA on weeks 3 and 6. Serum samples (n = 7/group) were collected for assay by ELISA for M1 antibody (squares) on week 3 and OVA antibody (triangles) on week 8. Data are combined from two independent experiments (n = 28 mice in total). Each individual point represents a single mouse, and the horizontal line is the median value. P values were calculated using a Kruskal-Wallis test with Dunn's procedure.

coupled to M1. *In vitro* delivery of OVA protein coupled to M1 enhanced T cell sensitivity to OVA by >10, 000-fold compared to that for OVA alone, M1 plus OVA, or OVA coupled to SMEZ-2 DM (Fig. 9a). Proliferating cells comprised both $CD4^+$ and $CD8^+$ T cells, and the proportion of these cells was similar irrespective of whether the stimulus was M1-OVA or OVA alone (data not shown).

Murine splenocytes (including those from MHC class II trans-

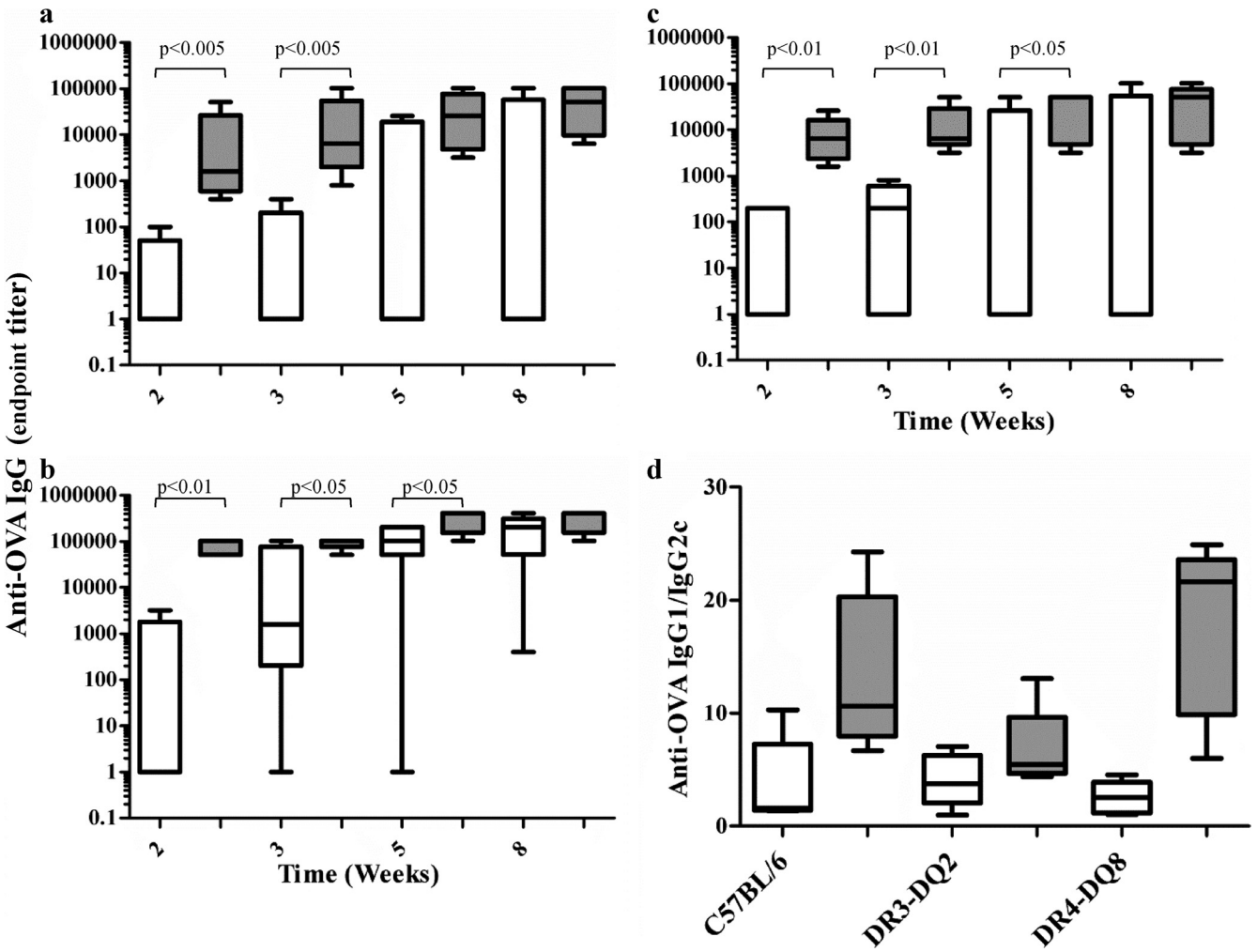

FIG 8 The M1 carrier enhances anti-OVA Ab responses in wild-type and transgenic mice. C57BL/6 (a), humanized DR3-DQ2 (b), or humanized DR4-DQ8 (c) transgenic mice were given a single subcutaneous injection with 10 μg OVA alone or 10 μg OVA coupled to M1 emulsified in IFA. The development of a circulating Ab response to OVA was determined by ELISA at 2, 3, 5, and 8 weeks postimmunization. (d) The ratio of IgG1 Ab/IgG2c Ab was measured by ELISA on week 8. All ELISA data are displayed as whisker plots showing the minimum to maximum range of data points, and the horizontal line represents the median value. Data shown contain 5 mice/treatment group and 30 mice in total and are representative of two independent experiments. *P* values were calculated using a one-tailed Mann-Whitney test.

genic animals) were harvested from multiple studies to measure specific T cell recall responses in M1-OVA-immunized mice relative to OVA-immunized control animals. The T cell proliferation responses in OVA-immunized mice were equivalent to those of the M1-OVA-immunized animals in all studies, as represented in Fig. 9b. OVA-specific IL-4 and IFN-γ splenocyte responses were measured by ELISPOT assay, with no striking differences observed between M1-OVA- and OVA-vaccinated mice (Fig. 9c). Thus, although the M1 carrier dramatically enhanced cellular responses to OVA *in vitro*, this was not matched by a corresponding increase in OVA-specific T cell expansion *in vivo*, despite a significantly enhanced and sustained T cell-dependent anti-OVA IgG1 response.

DISCUSSION

Vaccination is a highly successful strategy for stimulating protective immunity to microbial pathogens; however, there are numerous diseases which lack effective vaccines, including parasitic and bacterial diseases prevalent in the tropics (20) and influenza (14). Vaccine development has progressed from being based on heat-killed whole organisms or attenuated strains, which are intrinsically immunogenic, to refined preparations based on protein-, peptide-, or carbohydrate-based immunogens. A limitation of using defined vaccine preparations is that they are often poorly immunogenic, necessitating the need for an adjuvant, carrier, or specialized delivery system (32). An approach with considerable potential is direct delivery of materials to antigen-presenting cells by targeting cell surface molecules, This approach has been demonstrated with live vectors or specific targeting of receptor ligands and surface receptors (for example CD40, Gb3, and C-type lectins) with antibody (41).

We describe an alternative approach using a detoxified superantigen to target coupled antigen to MHC class II on antigen-presenting cells *in vitro* and *in vivo*. The key residues required for binding of the TCR and MHC class II were identified on the basis of the published structure of SEC3 (26), substituted, and con-

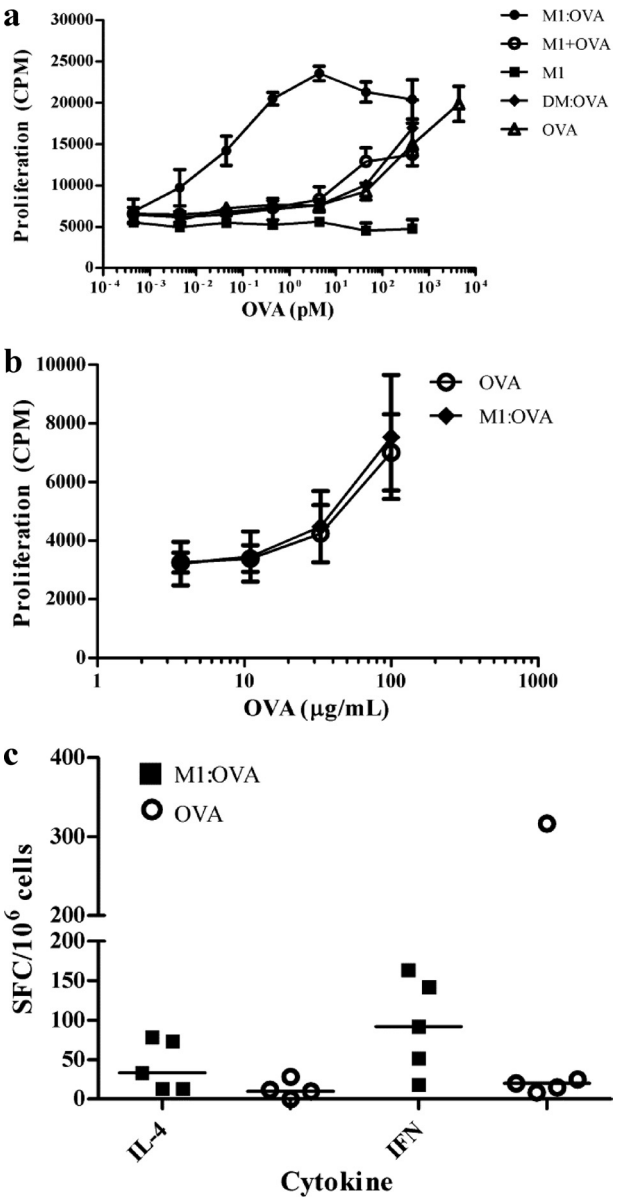

FIG 9 Conjugation of antigen to the M1 carrier enhances *in vitro* but not *in vivo* antigen-specific cellular responses. (a) Splenocytes from OVA-immunized BALB/c mice were cultured with graded doses of OVA, DM-OVA, M1, M1 plus OVA, and M1-OVA. Proliferation was quantified by the addition of [^{3}H]thymidine for the final 16 h of the 72-h culture period. Data are the mean ± SD of triplicate wells and are representative of two experiments. (b and c) Splenocytes were harvested from C57BL/6 mice 8 weeks after a single immunization with 10 μg OVA or M1-OVA. (b) Thymidine uptake was used to assay for proliferation in response to graded doses of OVA. Each mouse was assayed individually (n = 5/group; n = 10 mice in total per experiment), and data are presented as the mean ± SD. (c) ELISPOT assay was used to measure cytokine responses in response to 100 μg/ml OVA. Each point represents a single mouse (n = 5/group; n = 10 mice in total per experiment), with the median value represented as a horizontal line. All data are representative of two or more independent experiments.

firmed to eliminate superantigen-associated biological activities. Removal of the capacity to bind the TCR alone is sufficient to ablate mitogenic activities and release of proinflammatory cytokines responsible for superantigen toxicity.

Wild-type SMEZ-2 mainly stimulates hVβ8-bearing T cells and is the most potent superantigen identified in humans (33). Elimination of only two residues in the TCR binding site of SMEZ-2 produced M1 that was $>10^5$-fold less active in human T cell proliferation studies and failed to elicit any observable human T cell responses except at the highest concentration tested. This highlights the exquisitely small variations in TCR affinity that lead to either profound superantigen T cell activation or nothing at all. Some residual affinity of M1 toward soluble hVβ8 was detected by surface plasmon resonance biosensor analysis, but only at high ligand concentrations. This weak binding was clearly not sufficient to translate into T cell activation under normal physiological concentrations. Moreover, the antigen coupling point introduced on M1 is a cysteine deliberately engineered in the center of the TCR binding site to ensure that it does not interfere with MHC class II binding on the opposite face of M1, making it impossible for M1 to engage with TCR Vβ while antigen is bound.

Surface plasmon resonance studies also demonstrated that M1 retained specificity for MHC class II, and this was comparable to the finding for wild-type SMEZ-2. Specific binding to MHC class II was also evident on both murine and human antigen-presenting cells, leading to rapid internalization and colocalization with MHC class II protein in endocytic vesicles of dendritic cells. Antigen coupled to M1 is taken into a different intracellular compartment than antigen alone, and it has been speculated that it is taken up as part of the MHC class II recycling pathway (13). Lymph node tracking studies in mice showed that M1 was enriched in lymph nodes, which contain high numbers of MHC class II$^+$ antigen-presenting cells, corroborating data showing that M1 binds efficiently to all murine MHC class II$^+$ antigen-presenting cells, including all dendritic cell subsets in mice (13). M1 binding to dendritic cells *in vivo* does not elicit maturation of these cells (13).

In common with other superantigens, SMEZ-2 is much less active on mouse T cells. While the molecular basis for this potency is not entirely understood, it is most likely to be a consequence of the combined high affinities of SMEZ-2 for a peptide-dependent subset of HLA-DQ molecules and the human Vβ8 TCR polypeptide. The potency of SMEZ-2 increased approximately 100-fold in proliferation assays using cells from DR3-DQ2 or DR4-DQ8 transgenic mice, confirming the preference of SMEZ-2 for human DR/DQ proteins over mouse I-A/I-E. Production of the inflammatory cytokines CCL2, IL-6, and TNF-α in response to *in vivo* exposure to wild-type SMEZ-2 was also enhanced by up to 10-fold in DR3-DQ2 or DR4-DQ8 transgenic animals relative to nontransgenic animals. Selective expansion of Vβ11$^+$ T cells 3 days after exposure to wild-type SMEZ-2 (35, 44) was evident only in transgenic mice, reiterating the role of human MHC class II in maximal superantigen response. We speculate that the potency of SMEZ-2 could further approach that seen in humans if the mice were also transgenic for the human Vβ8 T cell receptor gene.

A strong, long-lasting IgG1 antibody response resulted from a single subcutaneous injection of M1-OVA or M1–$OVA_{323-339}$ conjugate in IFA. This was due entirely to the MHC class II binding of M1 because the mutant DM, which is defective in both TCR and MHC class II binding, conferred no enhanced immunity when coupled to OVA. Moreover, the effect was dependent on the physical attachment of OVA to M1. Immunization with unconjugated OVA and M1 was also ineffective. Mice transgenic for human MHC class II clearly responded more rapidly to the OVA-M1 conjugate and developed higher titers of anti-OVA antibody.

A potential limitation of a microbe-based conjugate is either the preexistence or development of antibodies in the recipient that might neutralize binding. M1 by itself was highly immunogenic, particularly in BALB/c mice. Nevertheless, BALB/c mice preimmunized and displaying strong anti-M1 seroconversion still developed an anti-OVA response equivalent to that of naïve mice when immunized with OVA-M1 conjugate. Thus, the effect of M1 conjugation was not compromised by preexisting immunity. Notably, normal human serum capable of neutralizing T cell proliferation in response to SMEZ-2 wild-type protein was unable to inhibit the binding of SMEZ-2 to MHC class II, suggesting that the immunodominant epitopes recognized by these antibodies are separated from the MHC class II binding site (Jacelyn Loh, personal communication). Wild-type SMEZ-2 is a highly potent superantigen on human cells but also efficiently targets MHC class II from other species such as the mouse, suggesting that the M1 carrier will be highly efficacious in humans, despite variability in HLA type.

Despite *in vitro* studies showing stimulation of greatly enhanced cellular proliferation of antigen-specific responder cells with M1-OVA, vaccination with M1-OVA or M1–$OVA_{323-339}$ failed to drive an observable *in vivo* T cell response. In these studies, IFA was used to deliver antigen. IFA is a water-oil emulsion that forms a slow-release depot rather than an emulsion that directly targets particular cell types or skews toward Th1 or Th2 immunity (9). The dominant subclass in the antibody response to OVA-M1 was IgG1, suggesting a predominantly Th2-type response. Stimulation of strong cellular immunity probably requires additional innate Toll-like receptor (TLR)-mediated signals not provided in IFA. It is worth noting that most antigen-targeting studies have used TCR transgenic animals such as OT-I and OT-II mouse systems for $OVA_{257-264}$ and $OVA_{323-339}$, respectively (4, 18), in order to increase precursor frequency sufficiently to observe T cell expansion. In a previous study, M1-OVA induced strong antitumor immunity in OT-I and OT-II mice when combined with the potent invariant NK T cell ligand α-galactosylceramide (13).

These studies clearly demonstrate that targeted mutation of the TCR binding site in the SMEZ-2 superantigen detoxified the protein, while it retained its capacity to bind MHC class II. Targeting of antigen to MHC class II-bearing cells has been shown previously using chemical coupling to anti-MHC class II antibodies (6) or by engineering T epitopes into the sequence of anti-MHC class II antibodies (29). Here we demonstrate a different strategy using conjugation to SMEZ-2 toxoid. This approach offers the advantage of cross-reactivity with both murine and human MHC class II, which permits experimentation in both systems. It is highly likely, given that the DR3-DQ2 and DR4-DQ8 mice appear to have an intermediate response to SMEZ-2 wild type, that the M1 carrier would be more effective in humans. The recombinant SMEZ-2 M1 protein can be readily produced in large quantities and is known to be temperature and protease resistant (3, 12, 19); hence, it is suited to *in vivo* applications. The mutations selected completely ablated superantigen-associated biological activities *in vivo* in both wild-type and humanized mice, resulting in the need for an adjuvant to demonstrate utility as a vaccine carrier. An alternative approach might be to partially retain superantigen-like activity, which is likely to produce an adjuvant effect; however, this strategy risks the prospect of residual toxic superantigen activities.

The M1 carrier merits further assessment to determine whether it is compatible with a variety of adjuvants. It may prove particularly useful in settings where elevated antibody responses are associated with protection, such as influenza (23) and *Streptococcus pyogenes* infection (21). Vaccination with M1 peptide produced significantly elevated antibody responses with 3-fold less peptide; thus, it may have potential in the context of epidemic influenza, in which antigen sparing may be a necessity to ensure sufficient vaccine coverage (40). Targeting antigen via MHC class II to antigen-presenting cells is an effective strategy to concentrate antigen to lymphoid organs, where it can be more efficiently presented to B cells to stimulate rapid and enhanced humoral immunity to conjugated peptide or protein antigen.

ACKNOWLEDGMENTS

This work was supported by the New Zealand Health Research Council, the Maurice Wilkins Centre for Molecular Biodiscovery, Auckland UniServices, and the Faculty of Medical and Health Sciences Research Development Fund.

We thank Kate Keech for her help in arranging the supply of the transgenic mice used in these studies. Justine Stewart and Chris Thoreaux arranged the importation and housing of the transgenic animals within FMHS at the University of Auckland. Fiona Clow provided assistance monitoring and maintaining the transgenic mice. Grant Munro gave helpful advice for this project. Reis Langley acquired the FPLC data on the M1–$OVA_{323-339}$ conjugate. Martin Middleditch from the University of Auckland Centre for Genomics and Proteomics arranged the mass spectrometry analysis and guidance on interpreting the data. The mouse anti-M1 monoclonal Ab was produced by Anuruddika Fernando. Surface plasmon resonance studies were performed by the University of Auckland Biacore Facility.

John D. Fraser holds a patent on the use of the SMEZ-2 M1 protein as a vaccine carrier.

REFERENCES

1. **Ada G, Isaacs D.** 2003. Carbohydrate-protein conjugate vaccines. Clin. Microbiol. Infect. **9**:79–85.
2. **Appel H, Gauthier L, Pyrdol J, Wucherpfennig KW.** 2000. Kinetics of T-cell receptor binding by bivalent HLA-DR. Peptide complexes that activate antigen-specific human T-cells. J. Biol. Chem. **275**:312–321.
3. **Balaban N, Rasooly A.** 2000. Staphylococcal enterotoxins. Int. J. Food Microbiol. **61**:1–10.
4. **Barnden MJ, Allison J, Heath WR, Carbone FR.** 1998. Defective TCR expression in transgenic mice constructed using cDNA-based alpha- and beta-chain genes under the control of heterologous regulatory elements. Immunol. Cell Biol. **76**:34–40.
5. **Bunch TA, Grinblat Y, Goldstein LS.** 1988. Characterization and use of the Drosophila metallothionein promoter in cultured Drosophila melanogaster cells. Nucleic Acids Res. **16**:1043–1061.
6. **Carayanniotis G, Barber BH.** 1987. Adjuvant-free IgG responses induced with antigen coupled to antibodies against class II MHC. Nature **327**:59–61.
7. **Chen Z, et al.** 2006. Humanized transgenic mice expressing HLA DR4-DQ3 haplotype: reconstitution of phenotype and HLA-restricted T-cell responses. Tissue Antigens **68**:210–219.
8. **Chen Z, et al.** 2002. A 320-kilobase artificial chromosome encoding the human HLA DR3-DQ2 MHC haplotype confers HLA restriction in transgenic mice. J. Immunol. **168**:3050–3056.
9. **Cox JC, Coulter AR.** 1997. Adjuvants—a classification and review of their modes of action. Vaccine **15**:248–256.
10. **DaSilva L, et al.** 2002. Humanlike immune response of human leukocyte antigen-DR3 transgenic mice to staphylococcal enterotoxins: a novel model for superantigen vaccines. J. Infect. Dis. **185**:1754–1760.
11. **Dellabona P, et al.** 1990. Superantigens interact with MHC class II molecules outside of the antigen groove. Cell **62**:1115–1121.
12. **Denny CB, Humber JY, Bohrer CW.** 1971. Effect of toxin concentration on the heat inactivation of staphylococcal enterotoxin A in beef bouillon and in phosphate buffer. Appl. Microbiol. **21**:1064–1066.
13. **Dickgreber N, et al.** 2009. Targeting antigen to MHC class II molecules

promotes efficient cross-presentation and enhances immunotherapy. J. Immunol. **182**:1260–1269.
14. **Fan J, et al.** 2004. Preclinical study of influenza virus A M2 peptide conjugate vaccines in mice, ferrets, and rhesus monkeys. Vaccine **22**:2993–3003.
15. **Finn A.** 2004. Bacterial polysaccharide-protein conjugate vaccines. Br. Med. Bull. **70**:1–14.
16. **Fraser JD, Proft T.** 2008. The bacterial superantigen and superantigen-like proteins. Immunol. Rev. **225**:226–243.
17. **Ho SN, Hunt HD, Horton RM, Pullen JK, Pease LR.** 1989. Site-directed mutagenesis by overlap extension using the polymerase chain reaction. Gene **77**:51–59.
18. **Hogquist KA, et al.** 1994. T cell receptor antagonist peptides induce positive selection. Cell **76**:17–27.
19. **Hoover DG, Tatini SR, Maltais JB.** 1983. Characterization of staphylococci. Appl. Environ. Microbiol. **46**:649–660.
20. **Hotez PJ, Ferris MT.** 2006. The antipoverty vaccines. Vaccine **24**:5787–5799.
21. **Huang YS, Fisher M, Nasrawi Z, Eichenbaum Z.** 2011. Defense from the group A Streptococcus by active and passive vaccination with the streptococcal hemoprotein receptor. J. Infect. Dis. **203**:1595–1601.
22. **Inaba K, et al.** 1992. Generation of large numbers of dendritic cells from mouse bone marrow cultures supplemented with granulocyte/macrophage colony-stimulating factor. J. Exp. Med. **176**:1693–1702.
23. **Karlsson Hedestam GB, et al.** 2008. The challenges of eliciting neutralizing antibodies to HIV-1 and to influenza virus. Nat. Rev. Microbiol. **6**:143–155.
24. **Laemmli UK.** 1970. Cleavage of structural proteins during the assembly of the head of bacteriophage T4. Nature **227**:680–685.
25. **Langley R, Patel D, Jackson N, Clow F, Fraser JD.** 2010. Staphylococcal superantigen super-domains in immune evasion. Crit. Rev. Immunol. **30**:149–165.
26. **Leder L, et al.** 1998. A mutational analysis of the binding of staphylococcal enterotoxins B and C3 to the T cell receptor beta chain and major histocompatibility complex class II. J. Exp. Med. **187**:823–833.
27. **Li PL, Tiedemann RE, Moffat SL, Fraser JD.** 1997. The superantigen streptococcal pyrogenic exotoxin C (SPE-C) exhibits a novel mode of action. J. Exp. Med. **186**:375–383.
28. **Liu S, et al.** 1997. Removal of endotoxin from recombinant protein preparations. Clin. Biochem. **30**:455–463.
29. **Lunde E, Western KH, Rasmussen IB, Sandlie I, Bogen B.** 2002. Efficient delivery of T cell epitopes to APC by use of MHC class II-specific Troybodies. J. Immunol. **168**:2154–2162.
30. **Martin RM, Brady JL, Lew AM.** 1998. The need for IgG2c specific antiserum when isotyping antibodies from C57BL/6 and NOD mice. J. Immunol. Methods **212**:187–192.
31. **Maxwell JR, Campbell JD, Kim CH, Vella AT.** 1999. CD40 activation boosts T cell immunity in vivo by enhancing T cell clonal expansion and delaying peripheral T cell deletion. J. Immunol. **162**:2024–2034.
32. **Moingeon P, de Taisne C, Almond J.** 2002. Delivery technologies for human vaccines. Br. Med. Bull. **62**:29–44.
33. **Proft T, Moffatt SL, Berkahn CJ, Fraser JD.** 1999. Identification and characterization of novel superantigens from Streptococcus pyogenes. J. Exp. Med. **189**:89–102.
34. **Proft T, et al.** 2000. The streptococcal superantigen SMEZ exhibits wide allelic variation, mosaic structure, and significant antigenic variation. J. Exp. Med. **191**:1765–1776.
35. **Rajagopalan G, et al.** 2008. Evaluating the role of HLA-DQ polymorphisms on immune response to bacterial superantigens using transgenic mice. Tissue Antigens **71**:135–145.
36. **Renz H, Bradley K, Larsen GL, McCall C, Gelfand EW.** 1993. Comparison of the allergenicity of ovalbumin and ovalbumin peptide 323-339. Differential expansion of V beta-expressing T cell populations. J. Immunol. **151**:7206–7213.
37. **Shimonkevitz R, Colon S, Kappler JW, Marrack P, Grey HM.** 1984. Antigen recognition by H-2-restricted T cells. II. A tryptic ovalbumin peptide that substitutes for processed antigen. J. Immunol. **133**:2067–2074.
38. **Snapper CM, Paul WE.** 1987. Interferon-gamma and B cell stimulatory factor-1 reciprocally regulate Ig isotype production. Science **236**:944–947.
39. **Sriskandan S, et al.** 2001. Enhanced susceptibility to superantigen-associated streptococcal sepsis in human leukocyte antigen-DQ transgenic mice. J. Infect. Dis. **184**:166–173.
40. **Stohr K, Kieny MP, Wood D.** 2006. Influenza pandemic vaccines: how to ensure a low-cost, low-dose option. Nat. Rev. Microbiol. **4**:565–566.
41. **Tacken PJ, Torensma R, Figdor CG.** 2006. Targeting antigens to dendritic cells in vivo. Immunobiology **211**:599–608.
42. **Towbin H, Staehelin T, Gordon J.** 1979. Electrophoretic transfer of proteins from polyacrylamide gels to nitrocellulose sheets: procedure and some applications. Proc. Natl. Acad. Sci. U. S. A. **76**:4350–4354.
43. **Trombetta ES, Mellman I.** 2005. Cell biology of antigen processing in vitro and in vivo. Annu. Rev. Immunol. **23**:975–1028.
44. **Unnikrishnan M, et al.** 2002. The bacterial superantigen streptococcal mitogenic exotoxin Z is the major immunoactive agent of Streptococcus pyogenes. J. Immunol. **169**:2561–2569.
45. **Wallny HJ, Sollami G, Karjalainen K.** 1995. Soluble mouse major histocompatibility complex class II molecules produced in Drosophila cells. Eur. J. Immunol. **25**:1262–1266.
46. **Welcher BC, et al.** 2002. Lethal shock induced by streptococcal pyrogenic exotoxin A in mice transgenic for human leukocyte antigen-DQ8 and human CD4 receptors: implications for development of vaccines and therapeutics. J. Infect. Dis. **186**:501–510.
47. **Yoon S, et al.** 2001. Analysis of the in vivo dendritic cell response to the bacterial superantigen staphylococcal enterotoxin B in the mouse spleen. Histol. Histopathol. **16**:1149–1159.